 CMES, vol.74, no.2, pp.109-137, 2011

Slow Rotation of an Axially Symmetric Particle about Its Axis of Revolution Normal to One or Two Plane Walls

Yi W. Wan[1] **and Huan J. Keh**[2]

Abstract: The steady rotation of an axially symmetric particle about its axis of revolution normal to two plane walls at an arbitrary position between them in a viscous fluid is studied theoretically in the limit of small Reynolds number. The fluid is allowed to slip at the surface of the particle. A method of distribution of a set of spherical singularities along the axis of revolution inside a prolate particle or on the fundamental disk within an oblate particle is used to find the general solution for the fluid velocity distribution that satisfies the boundary conditions at the confining walls and at infinity. The slip condition at the particle surface is then satisfied by applying a boundary collocation technique to this general solution to numerically determine the unknown constants. The torque exerted on the particle by the fluid is calculated with good convergence behavior for various cases. For the rotation of a confined no-slip sphere, our torque results agree excellently with the available solutions in the literature. It is found that, for a spheroid with specified aspect ratio and particle-to-wall spacings, its boundary-corrected hydrodynamic torque decreases monotonically with an increase in its slip coefficient. For given wall-to-wall spacings, the hydrodynamic torque is minimal when the particle is situated midway between the two plane walls and increases monotonically when it approaches either of the walls. For fixed separation and slip parameters, the normalized torque increases with a decrease in its axial-to-radial aspect ratio, and the boundary effect on the rotation of an oblate spheroid can be very significant.

Keywords: Creeping flow, Axially symmetric particle, Prolate and oblate spheroids, Singularity method, Boundary collocation technique, Slip-flow surface, Hydrodynamic torque, Boundary effect

[1] Department of Chemical Engineering, National Taiwan University, Taipei, 10617, Taiwan, ROC
[2] Corresponding Author: Department of Chemical Engineering, National Taiwan University, Taipei, 10617, Taiwan, ROC. E-mail: huan@ntu.edu.tw

1 Introduction

Problems concerning the motion of small particles through a viscous fluid at small Reynolds numbers have continued to receive much attention from investigators in the fields of chemical, biomedical, and environmental engineering and science. These moving phenomena are fundamental in nature, but permit one to develop rational understanding of many practical systems and industrial processes such as sedimentation, flotation, coagulation, meteorology, motion of cells in blood vessels, and rheology of suspensions. The theoretical study of this subject grew out of the classic work of Stokes (1951) for a rigid sphere with a no-slip surface moving in an unbounded, incompressible, Newtonian fluid. Oberbeck (1876) and Jeffery (1915) extended this result to the translation of an ellipsoid and the rotation of a particle of revolution, respectively. Explicit expressions for the resistance experienced by a rigid, no-slip, slightly deformed sphere undergoing low-Reynolds-number translational and rotational motions in a viscous fluid were derived to the first order in the small parameter characterizing the deformation from the spherical shape [Brenner (1964a)]. On the other hand, the creeping flow caused by the motion of a no-slip particle of more general shape has been treated semi-numerically by the boundary collocation method [Gluckman, Weinbaum, and Pfeffer (1972); Hsu and Ganatos (1989)], singularity method [Chwang and Wu (1975); Keh and Tseng (1994)], and boundary integral (boundary element) method [Youngren and Acrivos (1975); Sellier (2008)].

In the general formulation of the Stokes problems, it is usually assumed that no slippage arises at the solid-fluid interfaces. This assumption is well supported by experimental evidences at macroscopic scales, but it is not accepted physically at microscopic scales [Thompson and Troian (1997); Pit, Hervet, and Leger (2000); Martini et al. (2008); Cottin-Bizonne et al. (2008)]. The phenomenon that the adjacent fluid can slip frictionally over a solid surface occurs for cases such as the low-density gas flow around an aerosol particle [Ying and Peters (1991); Keh and Shiau (2000); Sharipov and Kalempa (2003)], the liquid flow near a lyophobic surface [Churaev, Sobolev, and Somov (1984); Tretheway and Meinhart (2002); Neto et al. (2005)], the micropolar fluid flow past a rigid particle [Sherif, Faltas, and Saad (2008)], and the viscous fluid flow over the surface of a porous medium [Saffman (1971); Bhattacharyya (2010); Keh and Keh (2010)] or a small particle of molecular size [Hu and Zwanzig (1974)]. Presumably, any such slipping would be proportional to the local shear stress of the fluid next to the solid surface [Felderhof (1977); Happel and Brenner (1983); Keh and Chen (1996)], known as Navier's slip [see Eq. (2)]. The constant of proportionality, β^{-1}, is called the slip coefficient of the solid surface.

The classic formula for the torque exerted by the ambient fluid of viscosity η on a

rotating rigid sphere of radius a with a slip-flow boundary condition at its surface, first derived by Basset (1961), is

$$T = 8\pi\eta a^3\Omega\frac{\beta a}{\beta a+3\eta}, \tag{1}$$

where Ω is the angular velocity of the particle. The quantity η/β is a slip length defined by Navier and Maxwell and extensively used in the literature. It can be pictured by noting that the fluid motion is the same as if the solid surface was displaced inward by a distance η/β with the velocity gradient extending uniformly right up to no-slip velocity at the surface. In the limiting case of the slip parameter $\eta/\beta a = 0$, there is no slip at the particle surface and Eq. (1) degenerates to the well-known Stokes result. When $\eta/\beta a \to \infty$, there is full slip at the particle surface and the torque vanishes. Recently, the low-Reynolds-number motion of a rigid sphere with an inhomogeneous slip boundary condition was also analyzed by a perturbation method [Willmott (2008)].

The resistance experienced by a full-slip spheroid undergoing uniform rotation in a viscous fluid was computed numerically by fitting the slip condition approximately with a general solution of the Stokes equations in the form of an infinite series expansion of spheroidal harmonics [Hu and Zwanzig (1974)]. Recently, the problem of rotation of an axially symmetric particle with an arbitrary slip coefficient about its axis of revolution in a viscous fluid was studied by using a singularity method based on the principle of distribution of a set of spherical singularities along the axis of revolution within a prolate particle or on the fundamental plane inside an oblate particle [Wan and Keh (2009)] and by using both a separable general solution in the form of an infinite series in spheroidal coordinates and the boundary collocation method [Chang and Keh (2011)]. The Stokes translation and rotation of a rigid particle which departs but little in shape from a sphere with the slip boundary condition were also analyzed, and explicit expressions for the hydrodynamic drag force and torque experienced by it were obtained to the second order in the small parameter characterizing the deformation [Senchenko and Keh (2006); Chang and Keh (2009)].

In practical applications of colloidal motion, particles are not isolated and will move in the presence of neighboring boundaries. Therefore, the boundary effects on creeping motions of rigid particles experiencing slip are of importance. Although the boundary effects on slow rotation of no-slip particles were studied in the past for several geometries [Jeffery (1915); Brenner (1962, 1964b); Brenner and Sonshine (1964); Hsu and Ganatos (1989)], these effects have not been investigated for the case of slip particles. In this article we use the method of distributed internal singularities incorporated with the boundary collocation technique [Keh

and Huang (2004); Keh and Chang (2010)] to analyze the creeping flow generated by an axially symmetric particle with an arbitrary slip coefficient rotating about its axis of revolution perpendicular to two plane walls at an arbitrary position between them; the particle can be either prolate or oblate. With this approach the torque exerted on a spheroid by the ambient fluid as functions of the slip parameter, the relative separation distances from the walls, and the aspect ratio of the spheroid is semi-numerically calculated. For the special cases of a no-slip sphere, our results show excellent agreement with those available in the literature.

2 Mathematical description of the problem

In this section, we consider the steady creeping flow caused by an axially symmetric particle rotating with a constant angular velocity Ω in an incompressible, Newtonian fluid about its axis of revolution (z axis) normal to two infinite plane walls whose distances from the center of the particle are c and d, respectively ($d \geq c$ is set without loss in generality), as shown in Fig. 1. Here (ρ, ϕ, z) and (r, θ, ϕ) denote the circular cylindrical and spherical coordinate systems, respectively, with their origin lying at the center of the particle. The fluid may slip frictionally at the surface of the particle.

The fluid flow governed by the Stokes equations for the case of vanishingly low

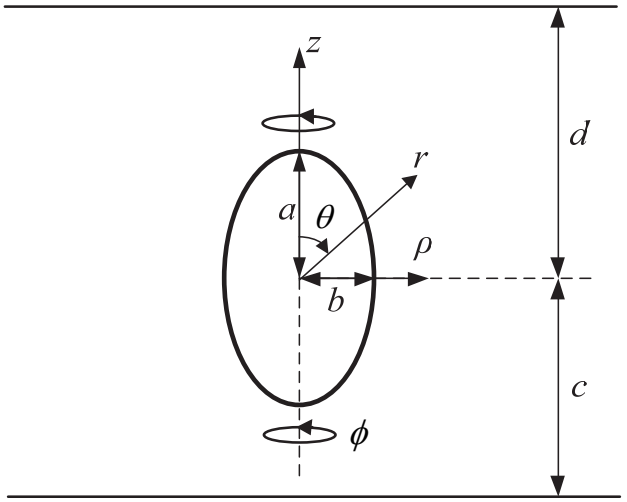

Figure 1: Geometrical sketch for the rotation of an axially symmetric particle about its axis of revolution perpendicular to two plane walls.

Reynolds number [Happel and Brenner (1983)] is axially symmetric and the only nonzero velocity component is v_ϕ in the ϕ direction. Because the relative tangential velocity of the fluid at the particle surface is proportional to the local tangential stress and the fluid is no-slip on the plane walls and motionless far from the particle, the boundary conditions are

$$v_\phi = \Omega\rho + \frac{1}{\beta}(n_\rho \tau_{\rho\phi} + n_z \tau_{z\phi}) \text{ on } S_p. \tag{2}$$

$$v_\phi = 0 \text{ at } z = -c,\ d, \tag{3}$$

$$v_\phi = 0 \text{ as } \rho \to \infty \text{ and } -c \le z \le d. \tag{4}$$

Here, $\tau_{\rho\phi}$ and $\tau_{z\phi}$ are the nonzero components of the viscous stress tensor in cylindrical coordinates,n_ρ and n_z are the local ρ and z components of the unit normal vector $\mathbf{n}$ on the particle surface S_p pointing into the fluid, and $1/\beta$ is the constant frictional-slip coefficient about the surface of the particle.

In order to solve for v_ϕ, a set of spherical singularities satisfying the Stokes equations and the boundary conditions in Eqs. (3) and (4) will be chosen and distributed along the axis of revolution inside a prolate particle or on the fundamental plane within an oblate particle [Keh and Tseng (1994)]. The flow field surrounding the particle is constructed by the superposition of the set of the spherical singularities and the boundary condition (2) on the particle surface can be satisfied by making use of the multipole collocation method.

The fluid velocity distribution caused by a spherical singularity at the point $\rho = 0$ and $z = h$ is

$$v_\phi = \sum_{n=2}^{\infty} B_n \gamma_n(\rho, z, h), \tag{5}$$

where γ_n are functions defined by Eq. (A1) in Appendix A, and B_n are unknown constants. From Eq. (5), the stress components in Eq. (2) can be obtained as

$$\tau_{\rho\phi} = \eta \sum_{n=2}^{\infty} B_n \alpha_n(\rho, z, h), \tag{6}$$

$$\tau_{z\phi} = \eta \sum_{n=2}^{\infty} B_n \beta_n(\rho, z, h), \tag{7}$$

where α_n and β_n are functions defined by Eqs. (A2) and (A3).

Equations (5)-(7) for the fluid velocity and stress fields caused by a spherical singularity and boundary condition (2) on the particle surface will be utilized in the following sections to solve for the hydrodynamic torque induced by the rotation of an axially symmetric particle about its axis of revolution perpendicular to two plane walls.

3 Solution for the rotation of a sphere normal to two plane walls

A spherical singularity described in the previous section is used in this section to obtain the solution for the rotation of a slip spherical particle of radius a about an axis normal to two plane walls. The flow field generated by the rotation of the sphere can be represented by a singularity placed at its center. Thus, the velocity and stress components for the fluid motion caused by the rotating sphere are given by Eqs. (5)-(7) with $h = 0$. To determine the unknown constants B_n, one can apply the boundary condition (2) at the particle surface to these velocity and stress components to yield

$$\sum_{n=2}^{\infty} B_n \gamma_n^*(\rho, z, 0) = \Omega\rho \text{ at } r = a, \tag{8}$$

where

$$\gamma_n^*(\rho, z, h) = \gamma_n(\rho, z, h) - \frac{\eta}{\beta}[n_\rho \alpha_n(\rho, z, h) + n_z \beta_n(\rho, z, h)]. \tag{9}$$

The torque acting on the particle by the fluid is [Wan and Keh (2009)]

$$T = 8\pi\eta B_2. \tag{10}$$

That is, only the lowest-order coefficient B_2 of the spherical singularity contributes to the hydrodynamic torque on the particle.

To satisfy the boundary condition (8) exactly along the entire half-circular generating arc of the sphere in a longitudinal plane (from $\theta = 0$ to $\theta = \pi$) would require the solution of the whole infinite array of the unknown constants B_n. However, the multipole collocation technique [Gluckman, Weinbaum and Pfeffer, (1972)] enforces the boundary condition at a finite number of discrete points on the particle's generating arc and truncates the infinite series in Eqs. (5)-(8) into finite ones. If the boundary is approximated by satisfying the condition (8) at N discrete points on the generating arc, then the infinite series are truncated after N terms, resulting in a system of N simultaneous linear algebraic equations in the truncated form of Eq. (8). This matrix equation can be solved by any matrix-reduction technique to yield the N unknown constants B_n required in the truncated equation for the fluid velocity distribution. The accuracy of the truncation technique can be improved to any degree by taking a sufficiently large value of N.

The details of the collocation scheme used for this work are given in a previous paper (Wan and Keh 2009). The numerical solutions of the dimensionless hydrodynamic torque $T/8\pi\eta a^3\Omega$ for the rotation of a sphere about an axis normal to a single plane wall (with $d \to \infty$) are presented in Table 1 for various values of the

dimensionless spacing parameter a/c and slip parameter $\eta/\beta a$ using the boundary collocation technique. All of the results obtained under this collocation scheme converge to at least five significant digits. The accuracy and convergence behavior of the truncation technique depends principally upon the relative spacing a/c. For the difficult case of $a/c = 0.999$, the number of collocation points with $N = 60$ is sufficiently large to achieve this convergence. Our collocation results for the no-slip case (with $\eta/\beta a = 0$) agree excellently with the numerical solutions obtained by Jeffery (1915) using spherical bipolar coordinates. As expected, the results in Table 1 illustrate that the torque on the sphere is a monotonic increasing function of a/c for any given value of $\eta/\beta a$. The normalized wall-corrected torque on the sphere decreases monotonically with an increase in $\eta/\beta a$ and vanishes at the limit $\eta/\beta a \to \infty$, keeping a/c unchanged.

Table 1: The dimensionless torque experienced by a sphere rotating about an axis normal to a single plane wall at various values of a/c and $\eta/\beta a$

a/c	$T/8\pi\eta a^3\Omega$			
	$\eta/\beta a = 0$	$\eta/\beta a = 0.1$	$\eta/\beta a = 1$	$\eta/\beta a = 10$
0.1	1.00013	0.76930	0.25001	0.03226
0.2	1.00100	0.76982	0.25006	0.03226
0.3	1.00339	0.77123	0.25021	0.03226
0.4	1.00807	0.77400	0.25050	0.03227
0.5	1.01593	0.77861	0.25098	0.03227
0.6	1.02800	0.78564	0.25170	0.03229
0.7	1.04579	0.79581	0.25271	0.03230
0.8	1.07186	0.81022	0.25405	0.03232
0.9	1.11221	0.83079	0.25578	0.03235
0.95	1.14331	0.84459	0.25680	0.03236
0.975	1.16519	0.85277	0.25734	0.03237
0.99	1.18310	0.85822	0.25768	0.03238
0.995	1.19092	0.86014	0.25779	0.03238
0.999	1.19901	0.86171	0.25791	0.03238

Some converged collocation solutions for the dimensionless torque $T/8\pi\eta a^3\Omega$ are presented in Table 2 for the rotation of a sphere about an axis perpendicular to two plane walls at two particular positions between them (with $c/(c+d) = 0.25$ and 0.5) for various values of the parameters a/c and $\eta/\beta a$. Analogous to the situation of rotation of a sphere normal to a single plane wall, for a constant value of $c/(c+d)$, the torque on the sphere rotating between two parallel walls increases monotonically with an increase in a/c for a fixed value of $\eta/\beta a$ and with a decrease

Table 2: The dimensionless torque experienced by a spherical particle rotating about an axis normal to two plane walls at various values of a/c, $c/(c+d)$, and $\eta/\beta a$

$c/(c+d)$	a/c	$T/8\pi\eta a^3\Omega$			
		$\eta/\beta a=0$	$\eta/\beta a = 0.1$	$\eta/\beta a=1$	$\eta/\beta a = 10$
0.25	0.1	1.00013	0.76931	0.25001	0.03226
	0.2	1.00102	0.76983	0.25006	0.03226
	0.3	1.00344	0.77126	0.25021	0.03226
	0.4	1.00819	0.77407	0.25051	0.03227
	0.5	1.01616	0.77874	0.25099	0.03227
	0.6	1.02841	0.78587	0.25172	0.03229
	0.7	1.04644	0.79620	0.25275	0.03230
	0.8	1.07286	0.81080	0.25411	0.03232
	0.9	1.11367	0.83164	0.25587	0.03235
	0.95	1.14506	0.84560	0.25690	0.03237
	0.975	1.16710	0.85387	0.25745	0.03237
	0.99	1.18510	0.85937	0.25779	0.03238
	0.995	1.19295	0.86131	0.25791	0.03238
	0.999	1.20107	0.86290	0.25803	0.03238
0.5	0.1	1.00023	0.76936	0.25001	0.03226
	0.2	1.00181	0.77030	0.25011	0.03226
	0.3	1.00612	0.77285	0.25038	0.03226
	0.4	1.01464	0.77786	0.25090	0.03227
	0.5	1.02901	0.78628	0.25177	0.03229
	0.6	1.05133	0.79920	0.25308	0.03231
	0.7	1.08457	0.81810	0.25492	0.03234
	0.8	1.13392	0.84514	0.25740	0.03238
	0.9	1.21143	0.88424	0.26060	0.03243
	0.95	1.27192	0.91071	0.26250	0.03245
	0.975	1.31480	0.92650	0.26349	0.03247
	0.99	1.35007	0.93704	0.26412	0.03248
	0.995	1.36553	0.94076	0.26438	0.03248
	0.999	1.38159	0.94382	0.26455	0.03248

in $\eta/\beta a$ (from zero at the limit $\eta/\beta a \to \infty$) for a given value of a/c.

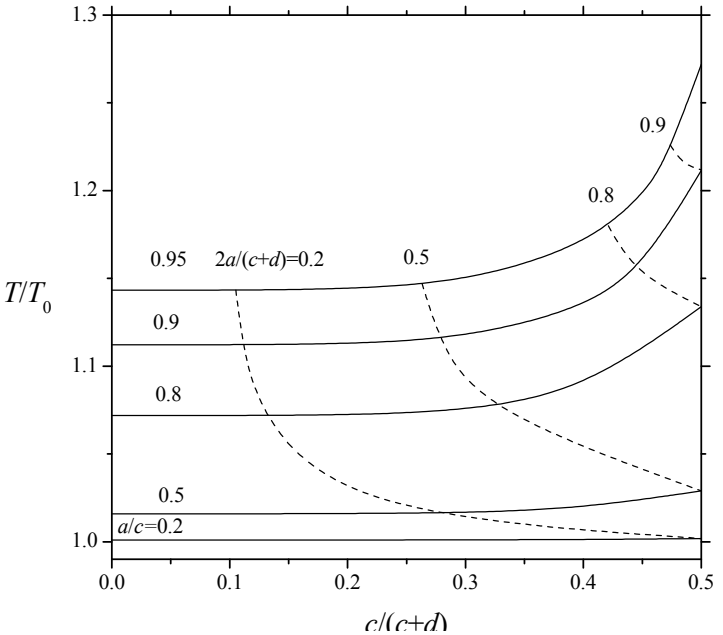

Figure 2: Plots of the normalized torque T/T_0 for the rotation of a no-slip sphere ($\eta/\beta a = 0$) about an axis perpendicular to two plane walls versus the ratio $c/(c+d)$ with a/c and $2a/(c+d)$ as parameters.

Figure 2 shows the collocation results for the hydrodynamic torque T exerted on a no-slip sphere ($\eta/\beta a = 0$) rotating about an axis perpendicular to two plane walls at various positions between them. The torque T_0 acting on an identical particle in an unbounded fluid (as $a/c \to \infty$) is used to normalize the boundary-corrected values. The solid curves (with a/c =constant) illustrate the effect of the position of the second wall (at $z = d$, where $d \geq c$) on the hydrodynamic torque for various specific values of the relative sphere-to-wall spacing c/a. Evidently, the approach of a second wall will enhance the hydrodynamic torque experienced by the particle in the vicinity of the first wall. The dashed curves [with $2a/(c+d)$ =constant] indicate the variation of the torque as a function of the particle position at various given values of the relative wall-to-wall spacing $(c+d)/2a$. At a constant value of $2a/(c+d)$, the sphere experiences a minimum hydrodynamic torque when it is located midway between the two plane walls [$c/(c+d) = 1/2$], and the torque increases monotonically as the particle approaches either of the walls. These ten-

dencies are also true for a slip particle with any finite value of $\eta/\beta a$, whose results are not presented here for conciseness but can also be obtained accurately.

The results of the normalized hydrodynamic torque T/T_0 exerted on a sphere rotating about an axis perpendicular to a single plane wall $[c/(c+d)=0]$ and to two equally distant plane walls $[c/(c+d)=1/2]$ as functions of the spacing parameter a/c for various values of $\eta/\beta a$ are plotted in Fig. 3. As expected, the value of T/T_0 increases monotonically with an increase in the ratio a/c from $T/T_0=1$ at $a/c=0$. The normalized wall-corrected torque on the sphere decreases with an increase in $\eta/\beta a$, keeping a/c unchanged. It can be seen from this figure (or from a comparison between Table 1 and Table 2) that, for an arbitrary combination of the parameters a/c and $\eta/\beta a$, the assumption that the results for two walls can be obtained by the simple addition of the single-wall effects always overestimates the correction to the hydrodynamic torque on a particle.

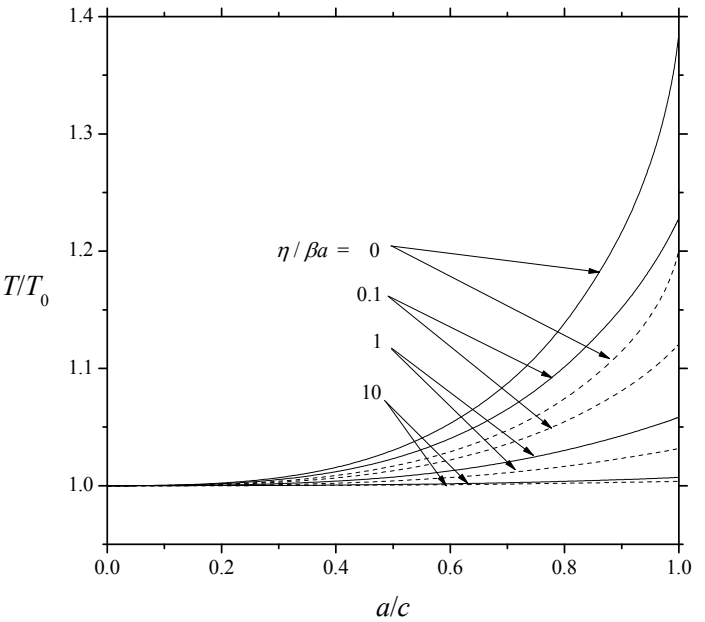

Figure 3: Plots of the normalized torque T/T_0 for the rotation of a sphere about an axis perpendicular to a single plane wall $[c/(c+d)\to 0$, dashed curves] and to two equally distant plane walls $[c/(c+d)=1/2$, solid curves] versus the separation parameter a/c for various values of the slip parameter $\eta/\beta a$.

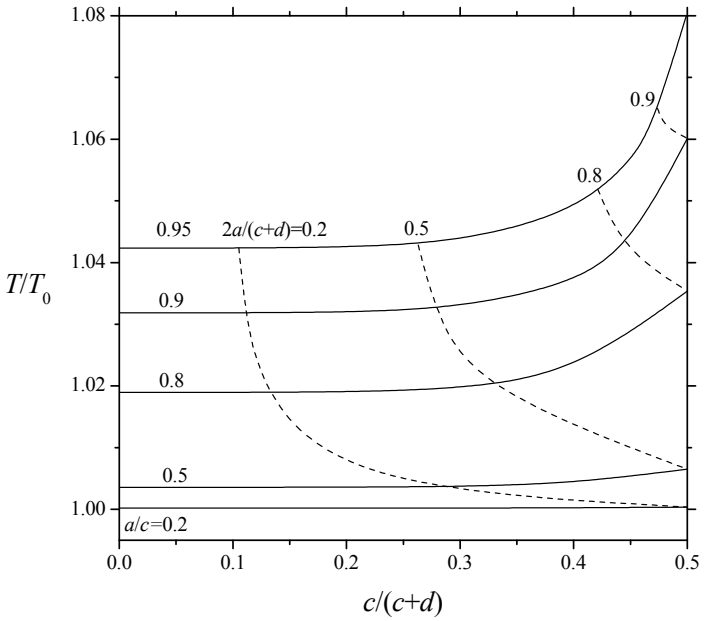

Figure 4: Plots of the normalized torque T/T_0 for the rotation of a no-slip prolate spheroid ($\eta/\beta b = 0$) with $a/b = 2$ about its axis of revolution perpendicular to two plane walls versus the ratio $c/(c+d)$ with a/c and $2a/(c+d)$ as parameters.

4 Axially symmetric rotation of prolate particles normal to two plane walls

In this section, we consider the rotation of a general prolate axisymmetric particle about its axis of revolution normal to two plane walls. A segment between points $\mathrm{A}(\rho = 0, z = -c_1)$ and $\mathrm{B}(\rho = 0, z = c_2)$ is taken along the axis of revolution inside the particle on which a set of spherical singularities are distributed (c_1 and c_2 are positive constants). The general solution of the fluid velocity can be constructed by the superposition of the spherical singularities distributed on the segment AB, and Eq. (5) is used to result in the integral form

$$v_\phi = \sum_{n=2}^{\infty} \int_{-c_1}^{c_2} B_n(t)\gamma_n(\rho, z, t)dt. \tag{11}$$

The corresponding integral expressions for the viscous stress components can be obtained accordingly using Eqs. (6) and (7). Equation (11) provides an exact solution for the Stokes equations that satisfies Eqs. (3) and (4), and the unknown density distribution function for the singularities, $B_n(t)$, must be determined from

the remaining boundary condition (2) using the multipole collocation technique. The torque acting on the particle by the fluid is obtained by the use of Eqs. (10) and (11), with the result

$$T = 8\pi\eta \int_{-c_1}^{c_2} B_2(t)\mathrm{d}t. \tag{12}$$

In order to use the collocation technique to satisfy the boundary condition at the particle surface, the integration encountered in Eqs. (11) and (12) need be treated numerically. Applying the M-point Gauss-Legendre quadrature formula of integration [Hornbeck (1975)] to Eq. (11) and truncating the infinite series after N terms, one obtains

$$v_\phi = \sum_{n=2}^{N+1} \sum_{m=1}^{M} B_{nm}\gamma_n(\rho, z, q_m), \tag{13}$$

where q_m are the quadrature zeros and B_{nm} are the unknown density constants. The corresponding quadrature expressions for the viscous stress components can also be obtained using Eqs. (6) and (7).

Application of the boundary condition (2) to Eq. (13) leads to

$$\sum_{n=2}^{N+1} \sum_{m=1}^{M} B_{nm}\gamma_n^*(\rho, z, q_m) = \Omega\rho \text{ on } S_\mathrm{p}, \tag{14}$$

where the functions γ_n^* are given by Eq. (9). The multipole collocation method allows the particle's boundary to be approximated by satisfying Eq. (14) at MN discrete values of z or θ on its surface and results in a set of MN simultaneous linear algebraic equations, which can be solved numerically to yield the MN density constants B_{nm} required in Eq. (13) for the fluid velocity distribution. Once these constants are determined, the torque exerted by the fluid on the particle can be obtained from Eq. (12) as

$$T = 8\pi\eta \sum_{m=1}^{M} B_{2m}. \tag{15}$$

5 Solution for the rotation of a prolate spheroid normal to two plane walls

The method presented in the previous section is used in this section to obtain the solution for the rotation of a slip prolate spheroid about its axis of revolution normal to one or two plane walls. The surface of a spheroid is represented in cylindrical coordinates by

$$z(\rho) = \pm\, a[1 - (\frac{\rho}{b})^2]^{1/2}, \tag{16}$$

where $0 \leq \rho \leq b$, and $-a \leq z \leq a$. For the case of a prolate spheroid, a and b are the major and minor semi-axes, respectively ($a > b > 0$).

In Section 3, the boundary collocation solutions for the rotation of a spherical particle about an axis normal to one or two plane walls were presented. We now use the same collocation scheme incorporated with the method of distribution of spherical singularities to obtain the corresponding solution for a prolate spheroid. Here, the values of c_1 and c_2 in Eqs. (11) and (12) are taken to be identical and equal to $(a^2 - b^2)^{1/2}$, the half distance between the two foci of the prolate spheroid. In Table 3, numerical results of the nondimensional hydrodynamic torque $T/8\pi\eta b^3\Omega$ for the rotation of a prolate spheroid about its axis of revolution perpendicular to a single plane wall [$c/(c+d) = 0$] are presented for various values of the aspect ratio a/b, spacing parameter a/c, and slip parameter $\eta/\beta b$. To achieve good convergence for the calculation of T, a larger value of N in Eqs. (13) and (14) is required when the particle is located closer to the plane wall, whereas a larger value of M is needed when the aspect ratio of the spheroid becomes larger. For the difficult case of $a/c = 0.999$ and $a/b = 10$, the number of collocation points with $N = 8$ and $M = 60$ is sufficiently large for the numerical results of the torque to converge to at least five significant figures.

Some collocation solutions of the dimensionless torque $T/8\pi\eta b^3\Omega$ for the rotation of a prolate spheroid about its axis of revolution perpendicular to two equally distant plane walls [$c/(c+d) = 1/2$] are presented in Table 4 for various values of a/b, a/c, and $\eta/\beta b$. Both Table 3 and Table 4 indicate that the boundary-corrected hydrodynamic torque (or viscous retardation) on the spheroid increases monotonically with an increase in a/c for fixed values of a/b and $\eta/\beta b$ and with a decrease in $\eta/\beta b$ for given values of a/b and a/c. This outcome is also true for a general case with any given value of $c/(c+d)$ other than 0 and 1/2, whose results are not presented here for conciseness but can also be obtained accurately.

The collocation results for the hydrodynamic torque T exerted on a no-slip prolate spheroid ($\eta/\beta b = 0$) with aspect ratio $a/b = 2$ rotating about its axis of revolution perpendicular to two plane walls at various positions between them normalized by the corresponding torque T_0 acting on the particle when the walls are not present (as $a/c \to \infty$) are illustrated in Fig. 4. Analogous to the corresponding case of a spherical particle discussed in Section 3, the approach of a second wall will enhance the hydrodynamic torque experienced by the spheroid in the vicinity of the first wall. At a constant value of $2a/(c+d)$, the spheroid experiences a minimum torque when it is located midway between the two plane walls [$c/(c+d) = 1/2$], and the torque increases monotonically as the particle approaches either of the walls. In general, for an arbitrary combination of the parameters a/b, a/c, and $\eta/\beta b$, the assumption that the results for two walls can be obtained by simple addition of the

Table 3: The dimensionless torque experienced by a prolate spherioid rotating about its axis of revolution normal to a single plane wall at various values of a/b, a/c and $\eta/\beta b$

a/c	$T/8\pi\eta b^3\Omega$									
	$\eta/\beta b=0$			$\eta/\beta b=1$			$\eta/\beta b=10$			
	$a/b=2$	$a/b=5$	$a/b=10$	$a/b=2$	$a/b=5$	$a/b=10$	$a/b=2$	$a/b=5$	$a/b=10$	
0.1	1.61339	3.53042	6.80471	0.44262	1.03937	2.04709	0.05889	0.14215	0.28250	
0.2	1.61368	3.53051	6.80475	0.44264	1.03938	2.04709	0.05889	0.14215	0.28250	
0.3	1.61450	3.53076	6.80487	0.44270	1.03940	2.04710	0.05889	0.14215	0.28250	
0.4	1.61616	3.53128	6.80512	0.44283	1.03945	2.04713	0.05890	0.14215	0.28250	
0.5	1.61911	3.53223	6.80556	0.44304	1.03953	2.04717	0.05890	0.14215	0.28250	
0.6	1.62395	3.53382	6.80631	0.44339	1.03966	2.04723	0.05891	0.14215	0.28250	
0.7	1.63166	3.53645	6.80755	0.44392	1.03987	2.04733	0.05891	0.14215	0.28250	
0.8	1.64394	3.54085	6.80965	0.44473	1.04020	2.04750	0.05893	0.14216	0.28250	
0.9	1.66472	3.54890	6.81355	0.44596	1.04077	2.04779	0.05895	0.14217	0.28251	
0.95	1.68169	3.55603	6.81711	0.44680	1.04121	2.04802	0.05896	0.14218	0.28251	
0.99	1.70387	3.56612	6.82238	0.44764	1.04171	2.04830	0.05898	0.14219	0.28252	
0.995	1.70820	3.56816	6.82350	0.44776	1.04179	2.04834	0.05898	0.14219	0.28252	
0.999	1.71263	3.57025	6.82466	0.44785	1.04185	2.04838	0.05898	0.14219	0.28252	

Table 4: The dimensionless torque experienced by a prolate spherioid rotating about its axis of revolution normal to two equally distant plane walls at various values of a/b, a/c and $\eta/\beta b$

	$T/8\pi\eta b^3\Omega$									
a/c	$\eta/\beta b = 0$				$\eta/\beta b = 1$				$\eta/\beta b = 10$	
	$a/b = 2$	$a/b = 5$	$a/b = 10$		$a/b = 2$	$a/b = 5$	$a/b = 10$		$a/b = 2$	$a/b = 5$	$a/b = 10$
0.1	1.61343	3.53042	6.80472		0.44262	1.03937	2.04709		0.05889	0.14215	0.28250
0.2	1.61395	3.53059	6.80479		0.44266	1.03939	2.04710		0.05889	0.14215	0.28250
0.3	1.61543	3.53105	6.80501		0.44277	1.03943	2.04712		0.05889	0.14215	0.28250
0.4	1.61846	3.53200	6.80545		0.44300	1.03951	2.04716		0.05890	0.14215	0.28250
0.5	1.62386	3.53374	6.80626		0.44339	1.03965	2.04723		0.05891	0.14215	0.28250
0.6	1.63281	3.53668	6.80764		0.44403	1.03989	2.04735		0.05892	0.14216	0.28250
0.7	1.64719	3.54159	6.80996		0.44501	1.04028	2.04754		0.05893	0.14216	0.28251
0.8	1.67044	3.54992	6.81394		0.44652	1.04092	2.04785		0.05896	0.14217	0.28251
0.9	1.71034	3.56538	6.82144		0.44883	1.04199	2.04840		0.05900	0.14219	0.28253
0.95	1.74333	3.57927	6.82837		0.45044	1.04283	2.04885		0.05902	0.14221	0.28254
0.99	1.78688	3.59910	6.83874		0.45204	1.04381	2.04939		0.05905	0.14222	0.28254
0.995	1.79544	3.60314	6.84096		0.45227	1.04396	2.04947		0.05905	0.14223	0.28254
0.999	1.80422	3.60728	6.84326		0.45245	1.04409	2.04955		0.05906	0.14223	0.28254

single-wall effects overestimates the correction to the hydrodynamic torque on a spheroid.

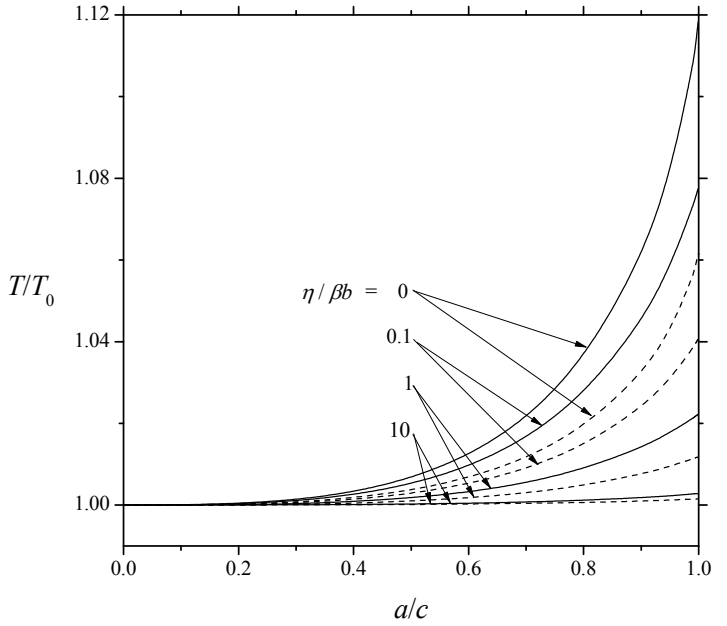

Figure 5: Plots of the normalized torque T/T_0 for the rotation of a prolate spheroid with $a/b = 2$ about its axis of revolution perpendicular to a single plane wall [$c/(c+d) \to 0$, dashed curves] and to two equally distant plane walls [$c/(c+d) = 1/2$, solid curves] versus the separation parameter a/c for various values of the slip parameter $\eta/\beta b$.

In Fig. 5, results of the normalized hydrodynamic torque T/T_0 exerted on a prolate spheroid with aspect ratio $a/b = 2$ rotating about its axis of revolution perpendicular to a single plane wall [$c/(c+d) = 0$] and to two equally distant plane walls [$c/(c+d) = 1/2$] are plotted as functions of the spacing parameter a/c for various values of $\eta/\beta b$. For a spheroid with given values of a/b (cases other than $a/b = 2$ are not displayed here for conciseness) and $\eta/\beta b$, the value of T/T_0 equals unity at $a/c = 0$ and increases monotonically with an increase in the ratio a/c. This normalized torque decreases with an increase in $\eta/\beta b$, keeping a/b and a/c unchanged.

The normalized hydrodynamic torque T/T_0 for the rotation of a prolate spheroid about its axis of revolution perpendicular to two equally distant plane walls [$c/(c+d) = 1/2$] as a function of its aspect ratio a/b for various values of the spacing

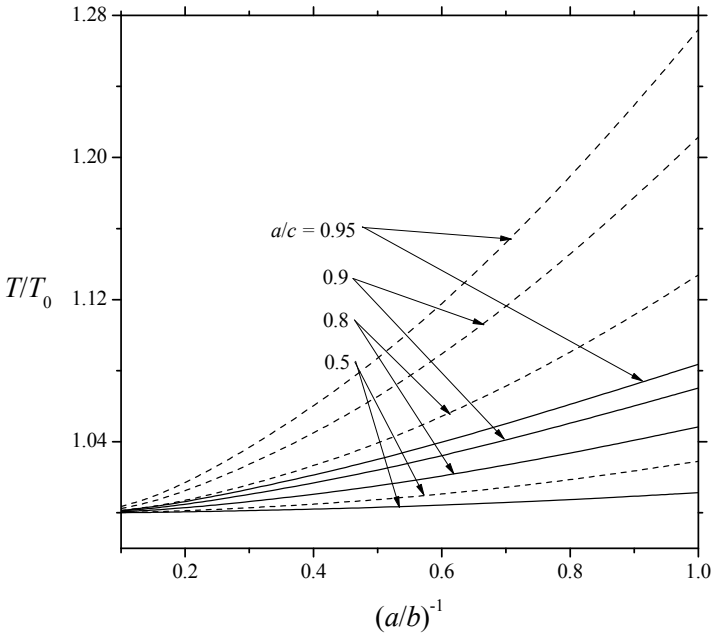

Figure 6: Plots of the normalized torque T/T_0 for the rotation of a prolate spheroid about an axis perpendicular to two equally distant plane walls $[c/(c+d) = 1/2]$ versus the inverse aspect ratio $(a/b)^{-1}$ for different values of the separation parameter a/c. The solid and dashed curves represent the cases with no slip ($\eta/\beta b = 0$) and with finite slip ($\eta/\beta b = 0.5$), respectively.

parameter a/c is plotted in Fig. 6. The solid and dashed curves represent the cases of rotation of a no-slip spheroid ($\eta/\beta b = 0$) and of a finite-slip spheroid (with $\eta/\beta b = 0.5$), respectively. It can be seen that, due to the decrease of the effective particle-boundary interaction area that offers hydrodynamic resistance to the rotation of the spheroid, T/T_0 decreases monotonically with an increase in the aspect ratio a/b for given values of a/c and $\eta/\beta b$. For fixed values of a/b and a/c, as expected, a no-slip spheroid experiences more hydrodynamic torque than a finite-slip spheroid does. Again, T/T_0 is a monotonically increasing function of a/c for specified values of a/b and $\eta/\beta b$.

6 Axially symmetric rotation of oblate particles normal to two plane walls

In Section 4, the rotational motion of a general prolate axisymmetric particle about its axis of revolution normal to two plane walls was considered and a set of spherical

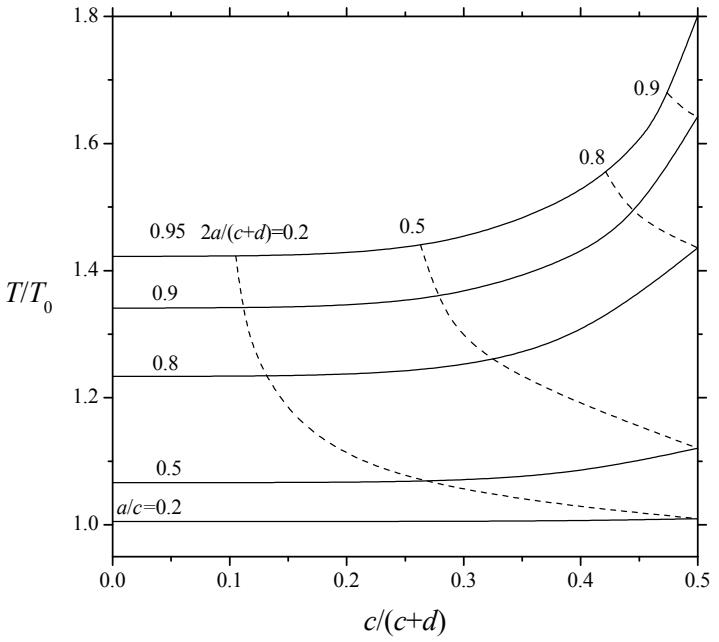

Figure 7: Plots of the normalized torque T/T_0 for the rotation of a no-slip oblate spheroid ($\eta/\beta b = 0$) with $a/b = 1/2$ about its axis of revolution perpendicular to two plane walls versus the ratio $c/(c+d)$ with a/c and $2a/(c+d)$ as parameters.

singularities must be distributed on a segment along the axis within the particle. In this section, we consider the corresponding rotation of a general oblate particle of revolution and the spherical singularities should be distributed on a fundamental circular disk S_d normal to and symmetric about the axis of revolution within the particle.

Let Q be an arbitrary point on S_d with the coordinates ($\rho = \hat{\rho}$, $\phi = \hat{\phi}$, $z = 0$). Then the fluid velocity at another point P($\rho = \rho$, $\phi = 0$, $z = z$) caused by a spherical singularity at Q can be obtained using Eq. (5),

$$\hat{v}_\phi = \frac{\rho - \hat{\rho}\cos\hat{\phi}}{\rho^*} \sum_{n=2}^{\infty} B_n \gamma_n(\rho^*, z, 0), \tag{17}$$

$$\hat{v}_\rho = \frac{\hat{\rho}\sin\hat{\phi}}{\rho^*} \sum_{n=2}^{\infty} B_n \gamma_n(\rho^*, z, 0), \tag{18}$$

where ρ^* is the distance from the point Q to the projection of the point P on the

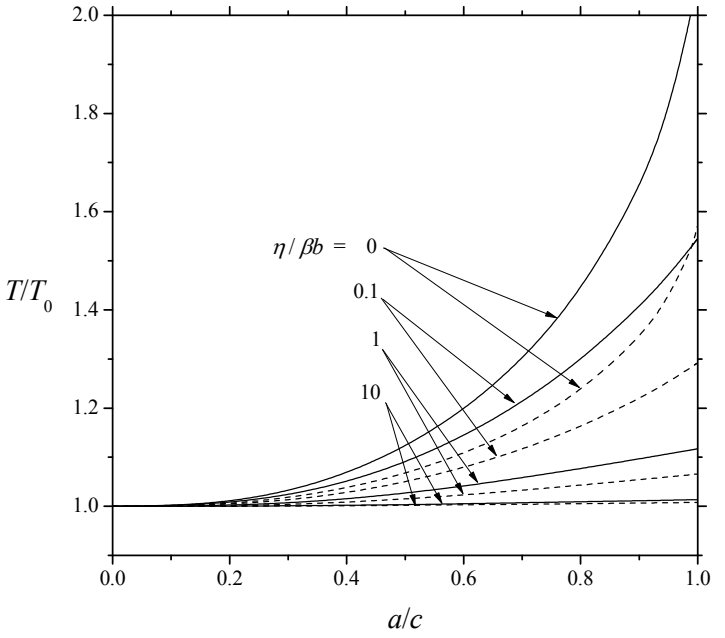

Figure 8: Plots of the normalized torque T/T_0 for the rotation of an oblate spheroid with $a/b = 1/2$ about its axis of revolution perpendicular to a single plane wall [$c/(c+d) \to 0$, dashed curves] and to two equally distant plane walls [$c/(c+d) = 1/2$, solid curves] versus the separation parameter a/c for various values of the slip parameter $\eta/\beta b$.

plane $z = 0$,

$$\rho^* = (\rho^2 + \hat{\rho}^2 - 2\rho\hat{\rho}\cos\hat{\phi})^{1/2}. \tag{19}$$

The fluid velocity distribution produced by the rotation of the confined oblate particle can be constructed by the superposition of the individual contributions in Eqs. (17) and (18) made by the entire set of singularities on the fundamental disk S_d. Thus, at an arbitrary location in the fluid, one has

$$v_\phi = \sum_{n=2}^{\infty} \int_0^{2\pi} \int_0^R \left(\frac{\rho - \hat{\rho}\cos\hat{\phi}}{\rho^*}\right) B_n(\hat{\rho}) \gamma_n(\rho^*, z, 0) \hat{\rho} d\hat{\rho} d\hat{\phi}, \tag{20}$$

where R is the radius of the disk S_d and the corresponding integral for v_ρ vanishes. Due to the axial symmetry of the system, the singularities ought to be distributed uniformly on each principal circle in S_d and the density distribution coefficients B_n

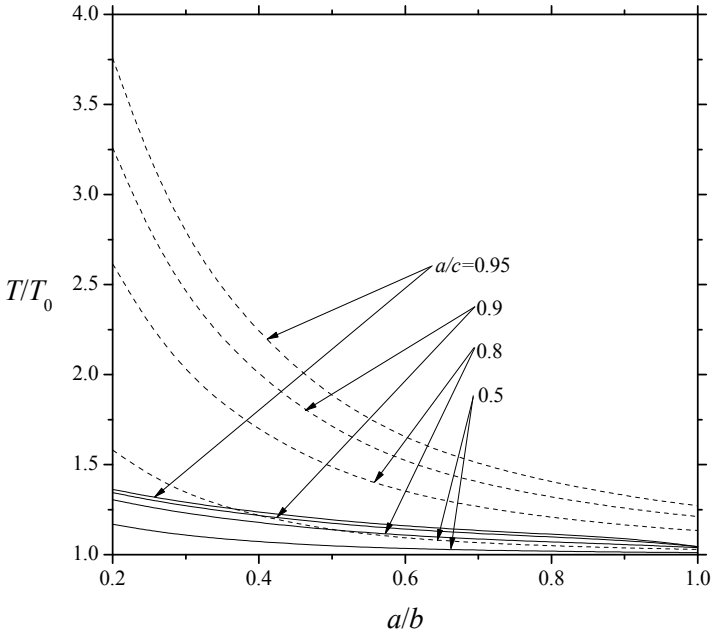

Figure 9: Plots of the normalized torque T/T_0 for the rotation of an oblate spheroid about an axis perpendicular to two equally distant plane walls $[c/(c+d) = 1/2]$ versus the aspect ratio a/b for different values of the separation parameter a/c. The solid and dashed curves represent the cases with no slip ($\eta/\beta b = 0$) and with finite slip ($\eta/\beta b = 0.5$), respectively.

are functions of $\hat{\rho}$ only. Equation (20) provides an exact solution for the Stokes equations that satisfies Eqs. (3) and (4), and the unknown density functions $B_n(\hat{\rho})$ must be determined from the remaining boundary condition (2) using the multipole collocation method. The corresponding integral expressions for the components of the viscous stress tensor can be obtained accordingly using Eqs. (6) and (7).

The torque acting on the oblate particle by the fluid can be obtained by using Eqs. (10) and (20), with the result

$$T = 16\pi^2\eta \int_0^R B_2(\hat{\rho})\hat{\rho}d\hat{\rho}. \tag{21}$$

Analogous to the case of a prolate particle examined in Section 4, the integration in Eq. (20) with respect to $\hat{\rho}$ can be performed by using the M-point Gauss-Legendre quadrature formula and the infinite series is truncated after N terms. With this

arrangement, Eq. (20) and the stress components in Eq. (2) become

$$v_\phi = \sum_{n=2}^{N+1} \sum_{m=1}^{M} B'_{nm} \gamma_{nm}(\rho, z, 0), \tag{22}$$

$$\begin{bmatrix} \tau_{\rho\phi} \\ \tau_{z\phi} \end{bmatrix} = \eta \sum_{n=2}^{N+1} \sum_{m=1}^{M} B'_{nm} \begin{bmatrix} \alpha_{nm}(\rho, z, 0) \\ \beta_{nm}(\rho, z, 0) \end{bmatrix}, \tag{23}$$

where the functions γ_{nm}, α_{nm}, and β_{nm} are defined by Eqs. (A7)-(A9) in Appendix A, and B'_{nm} are the unknown density constants.

Application of the boundary condition (2) to Eqs. (22) and (23) yields

$$\sum_{n=2}^{N+1} \sum_{m=1}^{M} B'_{nm} \gamma^*_{nm}(\rho, z, 0) = \Omega\rho \text{ on } S_\mathrm{p}, \tag{24}$$

where the function γ^*_{nm} is given by Eq. (9) with the subscript n of its functions being replaced by nm. Thus, the collocation technique described in Section 4 can be used to satisfy the boundary condition (24) and to determine the MN density constants B'_{nm} required for the fluid velocity distribution. Once these constants are determined, the hydrodynamic torque exerted on the particle can be obtained from Eq. (21) as

$$T = 16\pi^2 \eta \sum_{m=1}^{M} B'_{2m}. \tag{25}$$

7 Solution for the rotation of an oblate spheroid normal to two plane walls

The numerical solutions of the hydrodynamic torque experienced by a prolate spheroid rotating about its axis of revolution normal to one or two plane walls were presented in Section 5. In this section, the spherical singularity method and boundary collocation technique described in the previous section will be used to solve for the corresponding rotation of an oblate spheroid. The surface of the oblate spheroid can still be represented by Eqs. (16), but with $b > a > 0$. Now, the value of R in Eqs. (20) and (21) is taken to be $(b^2 - a^2)^{1/2}$, the radius of the focal circle of the oblate spheroid.

The numerical results of the nondimensional torque $T/8\pi\eta b^3\Omega$ for the rotation of an oblate spheroid about its axis of revolution perpendicular to a single plane wall $[c/(c+d) = 0]$ and to two equally distant plane walls $[c/(c+d) = 1/2]$ are presented in Tables 5 and 6, respectively, for various values of the aspect ratio a/b, spacing parameter a/c, and slip parameter $\eta/\beta b$. Again, the convergence behavior

of the method of spherical singularities in general is satisfactory. Analogous to Tables 3 and 4 for the corresponding confined rotation of a prolate spheroid, Tables 5 and 6 indicate that $T/8\pi\eta b^3\Omega$ increases monotonically with an increase in a/c for specified values of a/b, $c/(c+d)$, and $\eta/\beta b$ and with a decrease in $\eta/\beta b$ for constant values of a/b, $c/(c+d)$, and a/c.

Figure 7 presents the hydrodynamic torque T acting on a no-slip oblate spheroid ($\eta/\beta b = 0$) with $a/b = 1/2$ rotating about its axis of revolution perpendicular to two plane walls at various positions between them normalized by the corresponding torque T_0 acting on an unbounded oblate spheroid (as $a/c \to \infty$). Again, the approach of a second wall will enhance the torque exerted by the fluid on the spheroid in the vicinity of the first wall. At a constant value of $2a/(c+d)$, the particle experiences a minimum hydrodynamic torque when it is located midway between the two plane walls, and the torque increases monotonically as the particle approaches either of the walls.

The results of the normalized hydrodynamic torque T/T_0 experienced by an oblate spheroid with aspect ratio $a/b = 1/2$ rotating about its axis of revolution perpendicular to a single plane wall and to two equally distant plane walls as functions of a/c for various values of $\eta/\beta b$ are plotted in Fig. 8. Analogous to the case of a prolate spheroid discussed in Section 5, for an oblate spheroid with given aspect ratio (cases other than $a/b = 1/2$ are not illustrated here for conciseness), the value of T/T_0 increases monotonically with an increase in a/c from unity at $a/c = 0$ and decreases with an increase in $\eta/\beta b$, keeping the other parameters unchanged. It can be seen that the hydrodynamic torque exerted on the oblate spheroid can be very large when a/c is close to unity, especially as the value of $\eta/\beta b$ is small.

The normalized hydrodynamic torque T/T_0 for the rotation of an oblate spheroid about its axis of revolution perpendicular to two equally distant plane walls is plotted as a function of the aspect ratio a/b in Fig. 9 for different values of the spacing parameter a/c. The solid and dashed curves denote the cases of rotation of a no-slip spheroid ($\eta/\beta b = 0$) and of a finite-slip spheroid (with $\eta/\beta b = 0.5$), respectively. Similarly to the boundary effects on the motion of a prolate spheroid, T/T_0 for a confined oblate spheroid increases monotonically as the ratio a/b decreases or a/c increases, keeping other factors fixed. Again, a no-slip spheroid experiences more hydrodynamic torque than a finite-slip spheroid does for specified values of a/b and a/c.

8 Concluding remarks

In this work, the slow rotational motion of an axially symmetric particle about its axis of revolution normal to one or two plane walls in a viscous fluid, which

Table 5: The dimensionless torque experienced by an oblate spherioid rotating about its axis of revolution normal to a single plane wall at various values of a/b, a/c and $\eta/\beta b$

	$T/8\pi\eta b^3\Omega$									
a/c	$\eta/\beta b = 0$			$\eta/\beta b = 1$			$\eta/\beta b = 10$			
	a/b = 0.5	a/b = 0.3	a/b = 0.2	a/b = 0.5	$a/b = 0.3$	a/b = 0.2	a/b = 0.5	a/b = 0.3	a/b = 0.2	
0.1	0.70551	0.59211	0.53830	0.15956	0.12716	0.11297	0.02011	0.01594	0.01419	
0.2	0.70875	0.60120	0.55830	0.15973	0.12759	0.11389	0.02011	0.01595	0.01420	
0.3	0.71680	0.62062	0.59445	0.16014	0.12850	0.11547	0.02012	0.01597	0.01422	
0.4	0.73086	0.65007	0.64345	0.16087	0.12983	0.11734	0.02013	0.01599	0.01425	
0.5	0.75170	0.68923	0.70445	0.16190	0.13140	0.11922	0.02015	0.01601	0.01428	
0.6	0.78025	0.73896	0.77921	0.16321	0.13307	0.12097	0.02017	0.01603	0.01430	
0.7	0.81830	0.80215	0.87244	0.16474	0.13474	0.12255	0.02019	0.01606	0.01432	
0.8	0.86988	0.88549	0.99441	0.16642	0.13636	0.12396	0.02022	0.01608	0.01434	
0.9	0.94559	1.00644	1.17137	0.16820	0.13788	0.12521	0.02024	0.01610	0.01436	
0.95	1.00289	1.09813	1.30605	0.16911	0.13860	0.12578	0.02025	0.01611	0.01436	
0.99	1.07667	1.21720	1.48195	0.16984	0.13916	0.12621	0.02026	0.01611	0.01437	
0.995	1.09140	1.24119	1.51757	0.16993	0.13923	0.12627	0.02026	0.01611	0.01437	
0.999	1.1068	1.2664	1.5551	0.1700	0.1393	0.1263	0.0203	0.0161	0.0144	

Table 6: The dimensionless torque experienced by an oblate spherioid rotating about its axis of revolution normal to two equally distant plane walls at various values of a/b, a/c and $\eta/\beta b$

	$T/8\pi\eta b^3\Omega$								
a/c	$\eta/\beta b=0$			$\eta/\beta b=1$			$\eta/\beta b=10$		
	$a/b=0.5$	$a/b=0.3$	$a/b=0.2$	$a/b=0.5$	$a/b=0.3$	$a/b=0.2$	$a/b=0.5$	$a/b=0.3$	$a/b=0.2$
0.1	0.70590	0.59333	0.54142	0.15958	0.12721	0.11311	0.02011	0.01595	0.01419
0.2	0.71174	0.60964	0.57722	0.15988	0.12798	0.11473	0.02012	0.01596	0.01421
0.3	0.72625	0.64460	0.64236	0.16063	0.12960	0.11747	0.02013	0.01598	0.01425
0.4	0.75176	0.69810	0.73172	0.16191	0.13191	0.12067	0.02015	0.01602	0.01430
0.5	0.78992	0.77004	0.84450	0.16375	0.13463	0.12387	0.02018	0.01606	0.01435
0.6	0.84277	0.86260	0.98466	0.16607	0.13754	0.12684	0.02021	0.01610	0.01439
0.7	0.91411	0.98183	1.16188	0.16880	0.14044	0.12951	0.02025	0.01614	0.01442
0.8	1.01212	1.14122	1.39678	0.17180	0.14323	0.13189	0.02030	0.01617	0.01445
0.9	1.15815	1.37584	1.74189	0.17498	0.14586	0.13399	0.02034	0.01621	0.01447
0.95	1.26999	1.55560	2.00695	0.17660	0.14711	0.13495	0.02036	0.01622	0.01448
0.99	1.41526	1.79087	2.35537	0.17790	0.14807	0.13568	0.02038	0.01623	0.01449
0.995	1.44449	1.83850	2.42618	0.17807	0.14819	0.13577	0.02038	0.01624	0.01449
0.999	1.4752	1.8887	2.5010	0.1782	0.1483	0.1359	0.0204	0.0162	0.0145

may slip at the particle surface, is studied by the use of the method of internal singularity distributions combined with the boundary collocation technique. For the case of rotation of a prolate particle, a truncated set of spherical singularities is distributed along the axis inside the particle, whereas for the case of motion of an oblate particle, the singularities are placed on the fundamental disk of the particle. The numerical results for the torque exerted on the particle by the fluid indicate that the solution procedure converges rapidly and accurate solutions can be obtained for various cases of the particle shape, slippage, and separation from the walls. Although the numerical solutions were presented in the previous sections only for the rotation of a sphere, a prolate spheroid, and an oblate spheroid, the combined analytical and numerical technique utilized in this work can easily provide the hydrodynamic calculations for the rotation of a confined axisymmetric particle of other shapes, such as a prolate or oblate Cassini oval [Keh and Tseng (1994)].

In Tables 1-6 and Figs. 2-9, we presented only the results for the resistance problems, defined as those in which the torque T exerted by the surrounding fluid on the rotating particle is to be determined for a specified angular velocity Ω of the particle. In a mobility problem, on the other hand, the external torque T imposed on the particle is specified and the particle velocity Ω is to be determined. It is worth to note that our results can also be used for those physical problems in which the applied torque on the particle is the prescribed quantity and the particle must rotate accordingly.

Acknowledgement: Part of this research was supported by the National Science Council of the Republic of China.

Appendix A: Definitions of functions in Sections 2, 3, 4, and 6

For conciseness the definitions of some functions in Sections 2, 3, 4, and 6 are listed in this appendix. The functions appearing in Eqs. (5)-(7), (9), (11), (13), (17), (18), and (20) are defined as

$$\gamma_n(\rho,z,h) =$$
$$\int_0^\infty (\sinh\tau)^{-1}[\chi_n(\omega,d-h)\sinh\sigma-\chi_n(\omega,-c-h)\sinh\eta]\omega\, J_1(\omega\rho)\mathrm{d}\omega$$
$$+n\rho^{-1}(\rho^2+z_h^2)^{-(n-1)/2}G_n^{-1/2}(\kappa), \tag{A1}$$

$$\alpha_n(\rho,z,h) =$$

$$\int_0^\infty (\sinh\tau)^{-1}[\chi_n(\omega,-c-h)\sinh\eta-\chi_n(\omega,d-h)\sinh\sigma]\omega^2 J_2(\omega\rho)\mathrm{d}\omega$$

$$-n\rho^{-2}(\rho^2+z_h^2)^{-(n+2)/2}\{(\rho^2+z_h^2)^{1/2}[2z_h^2+(1+n)\rho^2]G_n^{-1/2}(\kappa)-z_h\rho^2 P_{n-1}(\kappa)\}, \tag{A2}$$

$$\beta_n(\rho,z,h)=$$
$$\int_0^\infty (\sinh\tau)^{-1}[\chi_n(\omega,d-h)\cosh\sigma-\chi_n(\omega,-c-h)\cosh\eta]\omega^2 J_1(\omega\rho)\mathrm{d}\omega$$
$$-n\rho^{-1}(\rho^2+z_h^2)^{-(n+2)/2}[(n-1)z_h(\rho^2+z_h^2)^{1/2}G_n^{-1/2}(\kappa)+\rho^2 P_{n-1}(\kappa)], \tag{A3}$$

where

$$\chi_n(\omega,z)=\frac{-1}{(n-1)!}(\frac{\omega|z|}{z})^{n-2}e^{-\omega|z|}, \tag{A4}$$

$$\sigma=\omega(z+c),\quad \eta=\omega(z-d),\quad \tau=\omega(c+d), \tag{A5}$$

$$\kappa=z_h(\rho^2+z_h^2)^{-1/2},\quad z_h=z-h, \tag{A6}$$

$G_n^{-1/2}$ is the Gegenbauer polynomial of the first kind of order n and degree –1/2, and P_n is the Legendre polynomial of order n.

The following are the definitions of some functions used in Eqs. (22) and (23) in Section 6:

$$\gamma_{nm}(\rho,z,h)=\int_0^{2\pi}(\frac{\rho-q_m\cos\hat{\phi}}{\rho_m^*})\gamma_n(\rho^*,z,h)d\hat{\phi}, \tag{A7}$$

$$\alpha_{nm}(\rho,z,h)=$$
$$\int_0^{2\pi}\{[\frac{q_m^2\sin^2\hat{\phi}}{(\rho_m^*)^3}-\frac{\rho-q_m\cos\hat{\phi}}{\rho\rho_m^*}]\gamma_n(\rho_m^*,z,h)+(\frac{\rho-q_m\cos\hat{\phi}}{\rho_m^*})^2\delta_n(\rho_m^*,z,h)\}d\hat{\phi}, \tag{A8}$$

$$\beta_{nm}(\rho,z,h)=\int_0^{2\pi}(\frac{\rho-q_m\cos\hat{\phi}}{\rho_m^*})\beta_n(\rho_m^*,z,h)d\hat{\phi}, \tag{A9}$$

where

$$\delta_n(\rho,z,h)=$$
$$\frac{1}{2}\int_0^\infty (\sinh\tau)^{-1}[\chi_n(\omega,d-h)\sinh\sigma-\chi_n(\omega,-c-h)\sinh\eta]\omega^2[J_0(\omega\rho)-J_2(\omega\rho)]\mathrm{d}\omega$$

$$-n\rho^{-2}(\rho^2+z_h^2)^{-(n+1)/2}[(n\rho^2+z_h^2)G_n^{-1/2}(\kappa)-\rho^2 P_{n-1}(\kappa)], \tag{A10}$$

$$\rho_m^* = (\rho^2+q_m^2-2\rho q_m\cos\hat{\phi})^{1/2}, \tag{A11}$$

and q_m are the Gauss-Legendre quadrature zeros. The integrations in Eqs. (A1)-(A3) and (A7)-(A10) can be performed numerically.

References

Basset, A. B. (1961): *A treatise on hydrodynamics, volume 2*. Dover, New York.

Bhattacharyya, A. (2010): Effect of momentum transfer condition at the interface of a model of creeping flow past a spherical permeable aggregate. *Eur. J. Mech. B/Fluids*, 29, 285-294.

Ahmadi, S.; Adams, B.L.; Fullwood, D.T. (2009): An Eulerian-Based Formulation for Studying the Evolution of the Microstructure under Plastic Deformations. *CMC: Computers, Materials & Continua*, vol.14, no.2, pp.141-169.

Brenner, H. (1962): Effect of finite boundaries on the Stokes resistance of an arbitrary particle. *J. Fluid Mech.*, 12, 35-48.

Brenner, H. (1964a): The Stokes resistance of a slightly deformed sphere. *Chem. Eng. Sci.*, 19, 519-539.

Brenner, H. (1964b): Slow viscous rotation of an axisymmetric body in a circular cylinder of finite length. *Appl. Sci. Res. (ser. A)*, 13, 81-120.

Brenner, H.; Sonshine, R. M. (1964): Slow viscous rotation of a sphere in a circular cylinder. *Quart. J. Mech. Appl. Math.*, 17, 55-63.

Chang, Y. C.; Keh, H. J. (2009): Translation and rotation of slightly deformed colloidal spheres experiencing slip. *J. Colloid Interface Sci.*, 330, 201-210.

Chang, Y. C.; Keh, H. J. (2011): Creeping-flow rotation of a slip spheroid about its axis of revolution. *Theor. Comput. Fluid Dyn.*, DOI: 10.1007/s00162-010-0216-4.

Chen, W.; Fu, Z.J.; Qin, Q.H. (2010): Boundary Particle Method with High-Order Trefftz Functions. *CMC: Computers, Materials & Continua*, vol.13, no.3, pp.201-217.

Churaev, N. V.; Sobolev, V. D.; Somov, A. N. (1984): Slippage of liquids over lyophobic solid surfaces. *J. Colloid Interface Sci.*, 97, 574-581.

Chwang, A. T.; Wu, T. Y. (1975): Hydrodynamic of low-Reynolds-number flow, Part 2. Singularity method for Stokes flows. *J. Fluid Mech.*, 67, 787-815.

Cottin-Bizonne, C.; Steinberger, A.; Cross, B.; Raccurt, O.; Charlaix, E. (2008): Nanohydrodynamics: The intrinsic flow boundary condition on smooth surfaces. *Langmuir*, 24, 1165-1172.

Felderhof, B. U. (1977): Hydrodynamic interaction between two spheres. *Physica*, 89A, 373-384.

Gluckman, M. J.; Weinbaum, S.; Pfeffer, R. (1972): Axisymmetric slow viscous flow past an arbitrary convex body of revolution. *J. Fluid Mech.*, 55, 677-709.

Happel, J.; Brenner, H. (1983): *Low Reynolds number hydrodynamics.* Nijhoff, The Netherlands.

Hornbeck, R. W. (1975): *Numerical Methods*. Quantum Publishers, New York.

Hsu, R.; Ganatos, P. (1989): The motion of a rigid body in viscous fluid bounded by a plane wall. *J. Fluid Mech.*, 207, 29-72.

Hu, C. M.; Zwanzig, R. (1974): Rotational friction coefficients for spheroids with the slipping boundary condition. *J. Chem. Phys.*, 60, 4354-4357.

Jeffery, G. B. (1915): On the steady rotation of a solid of revolution in a viscous fluid. *Proc. London Math. Soc.*, 14, 327-338.

Keh, H. J.; Chang, Y. C. (2010): Slow motion of a general axisymmetric slip particle along its axis of revolution and normal to one or two plane walls. *CMES: Computer Modeling in Engineering & Sciences*, vol. 62, no. 3, 225-253.

Keh, H. J.; Chen, S. H. (1996): The motion of a slip spherical particle in an arbitrary Stokes flow. *Eur. J. Mech., B/Fluids*, 15, 791-807.

Keh, H. J.; Huang, C. H. (2004): Slow motion of axisymmetric slip particles along their axes of revolution. *Int. J. Eng. Sci.*, 42, 1621-1644.

Keh, H. J.; Shiau, S. C. (2000): Effects of inertia on the slow motion of aerosol particles. *Chem. Eng. Sci.*, 42, 1621-1644.

Keh, H. J.; Tseng, C. H. (1994): Slow motion of an arbitrary axisymmetric body along its axis of revolution and normal to a plane surface. *Int. J. Multiphase Flow*, 20, 185-210.

Keh, M. P.; Keh, H. J. (2010): Slow motion of an assemblage of porous spherical shells relative to a fluid. *Transport Porous Med.*, 81, 261-275.

Martini, A.; Roxin, A.; Snurr, R. Q.; Wang, Q.; Lichter, S. (2008): Molecular mechanisms of liquid slip. *J. Fluid Mech.*, 600, 257-269.

Neto, C.; Evans, D. R.; Bonaccurso, E.; Butt, H. J.; Craig, V. S. J. (2005): Boundary slip in Newtonian liquids: a review of experimental studies. *Rep. Prog. Phys.*, 68, 2859-2897.

Oberbeck, A. (1876): Uber stationare Flussigkeitsbewegungen mit Berucksichtigung der inner Reibung. *J. Reine Angew. Math.*, 81, 62-80.

Pit, R.; Hervet, H.; Leger L. (2000): Direct experimental evidence of slip in hexadecane: solid interfaces. *Phys. Rev. Lett.*, 85, 980-983.

Saffman, P. G. (1971): On the boundary condition at the surface of a porous medium. *Studies Appl. Math.*, 50, 93-101.

Sellier, A. (2008): Slow viscous motion of a solid particle in a spherical cavity. *CMES: Computer Modeling in Engineering & Sciences*, vol. 25, no. 3, 165-179.

Senchenko, S.; Keh, H. J. (2006): Slipping Stokes flow around a slightly deformed sphere. *Phys. Fluids*, 18, 088104-1-4.

Sharipov, F.; Kalempa, D. (2003): Velocity slip and temperature jump coefficients for gaseous mixtures. I. Viscous slip coefficient. *Phys. Fluids*, 15, 1800-1806.

Sherif, H. H.; Faltas, M. S.; Saad, E. I. (2008): Slip at the surface of a sphere translating perpendicular to a plane wall in micropolar fluid. *Z. Angew. Math. Phys.*, 59, 293-312.

Stokes, G. G. (1851): On the effect of the internal friction of fluid on pendulums. *Trans. Cambridge Phil. Soc.*, 9, 8-106.

Thompson, P. A.; Troian, S. M. (1997): A general boundary condition for liquid flow at solid surfaces. *Nature*, 389, 360-362.

Tretheway, D. C.; Meinhart, C. D. (2002): Apparent fluid slip at hydrophobic microchannel walls. *Phys. Fluids*, 14, L9-L12.

Willmott, G. (2008): Dynamics of a sphere with inhomogeneous slip boundary conditions in Stokes flow. *Phys. Rev. E*, 77, 055302-1-4.

Ying, R.; Peters, M. H. (1991): Interparticle and particle-surface gas dynamic interactions. *Aerosol Sci. Technol.*, 14, 418-433.

Youngren, G. K.; Acrivos, A. (1975): Stokes flow past a particle of arbitrary shape: a numerical method of solution. *J. Fluid Mech.*, 69, 377-403.